

OPEN

# Effect of Immune Activation during Early Gestation or Late Gestation on Inhibitory Markers in Adult Male Rats

Tasnim Rahman<sup>1,2</sup>, Cynthia Shannon Weickert<sup>1,2,3</sup>, Lauren Harms<sup>4,5,6</sup>, Crystal Meehan<sup>4,5,6,7</sup>, Ulrich Schall<sup>5,6,8</sup>, Juanita Todd<sup>4,5,6</sup>, Deborah M. Hodgson<sup>4,5,6</sup>, Patricia T. Michie<sup>4,5,6</sup> & Tertia Purves-Tyson<sup>1,2\*</sup>

People with schizophrenia exhibit deficits in inhibitory neurons and cognition. The timing of maternal immune activation (MIA) may present distinct schizophrenia-like phenotypes in progeny. We investigated whether early gestation [gestational day (GD) 10] or late gestation (GD19) MIA, via viral mimetic polyI:C, produces deficits in inhibitory neuron indices (GAD1, PVALB, SST, SSTR2 mRNAs) within cortical, striatal, and hippocampal subregions of male adult rat offspring. *In situ* hybridisation revealed that polyI:C offspring had: (1) SST mRNA reductions in the cingulate cortex and nucleus accumbens shell, regardless of MIA timing; (2) SSTR2 mRNA reductions in the cortex and striatum of GD19, but not GD10, MIA; (3) no alterations in cortical or striatal GAD1 mRNA of polyI:C offspring, but an expected reduction of PVALB mRNA in the infralimbic cortex, and; (4) no alterations in inhibitory markers in hippocampus. Maternal IL-6 response negatively correlated with adult offspring SST mRNA in cortex and striatum, but not hippocampus. These results show lasting inhibitory-related deficits in cortex and striatum in adult offspring from MIA. SST downregulation in specific cortical and striatal subregions, with additional deficits in somatostatin-related signalling through SSTR2, may contribute to some of the adult behavioural changes resulting from MIA and its timing.

Neural activity between the cortex and striatum regulates motor, cognitive, and limbic function, and aspects of these modalities are perturbed in people with schizophrenia<sup>1,2</sup>. This neural activity is influenced by local inhibitory neurons, and the dysregulation of inhibition is postulated as a central contributor in the development of schizophrenia. Inhibitory tone is mainly established during early neurodevelopment to coordinate efficient neurotransmission<sup>3,4</sup>. Inhibitory interneurons migrate from the ganglionic eminence and the subventricular zone through the white matter to reach their destination in the cortical grey matter (see<sup>5</sup> for review) and hippocampus (see<sup>6</sup> for review). Striatal neurons are largely generated from the ganglionic eminences<sup>7</sup>. Perturbations during this neurodevelopmental epoch is therefore postulated to dysregulate inhibitory tone in the brain<sup>8</sup> and contribute to the behavioural phenotypes in schizophrenia (see<sup>9,10</sup> for review).

Glutamate decarboxylase-1 (GAD1) is one of the enzymes that catalyses the main inhibitory neurotransmitter in the brain, gamma-aminobutyric acid (GABA)<sup>11</sup>. There are two main subsets of GABAergic neurons that are distinguished based on their expression of the calcium-binding protein, parvalbumin (PVALB), or the neuropeptide hormone, somatostatin (SST) (see<sup>12</sup> for review). Studies in post-mortem human brain show that schizophrenia cases have reduced cortical<sup>13</sup>, hippocampal<sup>14,15</sup>, and striatal<sup>16,17</sup> GABAergic indices that suggest that these regions may contribute to the cognitive deficits exhibited by people with schizophrenia. The most consistently reported inhibitory deficits in the cortex of people with schizophrenia include reductions in GAD1<sup>18,19</sup>, PVALB<sup>8,20</sup>,

<sup>1</sup>School of Psychiatry, Faculty of Medicine, University of New South Wales, Sydney, NSW, Australia. <sup>2</sup>Neuroscience Research Australia, Sydney, NSW, Australia. <sup>3</sup>Department of Neuroscience and Physiology, Upstate Medical University, Syracuse, NY, USA. <sup>4</sup>School of Psychology, The University of Newcastle, Sydney, NSW, Australia. <sup>5</sup>Priority Centre for Brain and Mental Health Research, The University of Newcastle, Newcastle, NSW, Australia. <sup>6</sup>Hunter Medical Research Institute, Newcastle, NSW, Australia. <sup>7</sup>Division of Psychology, School of Medicine, College of Health and Medicine, University of Tasmania, Hobart, TAS, Australia. <sup>8</sup>School of Medicine and Public Health, The University of Newcastle, Newcastle, NSW, Australia. \*email: [t.purves-tyson@neura.edu.au](mailto:t.purves-tyson@neura.edu.au)

and SST<sup>8,21–24</sup> mRNAs. SST also elicits inhibition via somatostatin receptors (see<sup>25</sup> for review), and decreases in SST receptor 2 (*SSTR2*) mRNA is reported in the dorsolateral prefrontal cortex (dlPFC) of people with schizophrenia<sup>26</sup>. Whether it is proliferation, differentiation, migration, survival and/or function of these inhibitory neurons that contribute to schizophrenia pathophysiology is unclear.

One way to test the gap in knowledge regarding the origin of inhibitory neuropathology involves recapitulating epidemiological factors that increase the risk of schizophrenia in animal models. Epidemiological investigations show gestational and perinatal infection increases the risk of schizophrenia in progeny<sup>27–32</sup>. In rodent studies, maternal immune activation (MIA) can be induced in pregnant dams with the viral mimic polyribonucleoside:polyribocytidilic acid (polyI:C). This results in offspring (henceforth referred to as polyI:C offspring) that exhibit schizophrenia-like neuroanatomical changes at adulthood (such as reduced brain volume in cortical, striatal, and hippocampal regions<sup>33</sup>) and schizophrenia-like behavioural changes (such as deficits in sensorimotor gating<sup>34,35</sup>, increased amphetamine-induced hyperlocomotion<sup>34</sup>, and impaired learning<sup>36</sup>). This suggests MIA may contribute to neurobiological alterations in these brain regions in offspring. Indeed, reductions in GABA in cortex<sup>37</sup>, and *GAD1* mRNA in cortex and hippocampus<sup>38,39</sup> are found in polyI:C offspring. SST and PVALB neuron populations are trophically dependent on *trkB*<sup>40–43</sup>, and preliminary studies show alterations in the gene expression of *trkB* in the striatum of adult male polyI:C offspring<sup>44</sup>. This suggests that inhibitory neuron deficits may occur in the striatum of male polyI:C offspring.

The timing of MIA exposure is associated with distinct behavioural changes that may be associated with distinct neurobiological changes that contribute to these behaviours in offspring at adulthood<sup>45–47</sup>. Indeed, the timing of MIA exposure determines the extent and pattern of brain changes in foetal neurodevelopment (see<sup>48</sup> for review). In mice, early gestation MIA exposure results in offspring with behaviours that mimic positive symptoms of schizophrenia, and late gestation MIA exposure results in offspring with more negative and cognitive schizophrenia-like symptoms<sup>49</sup>. In rats, we found that early gestation MIA exposure results in male offspring with sensorimotor gating deficits, whilst late gestation MIA exposure results in male and female offspring with both sensorimotor gating and working memory deficits<sup>50</sup>. This suggests that the timing of MIA exposure on related neurobiological changes may be more apparent in male offspring versus female offspring.

Based on key neurotransmitter systems implicated in schizophrenia, our previous studies on the timing of MIA probed dopaminergic<sup>50</sup> and glutamatergic<sup>51</sup> indices in this model. For example, we recently reported that polyI:C offspring, from either early gestation MIA or late gestation MIA, exhibit glutamatergic alterations that are more pronounced in male offspring, and thus may relate to the sensorimotor gating deficits that are exacerbated in male polyI:C offspring<sup>51</sup>. Although studies in mice show that MIA is sufficient to reduce PVALB-positive cells in the medial prefrontal cortex in both early gestation and late gestation adult<sup>49,52</sup> and juvenile<sup>53</sup> polyI:C offspring, to our knowledge, there have been no studies on the effects of MIA, or the timing of MIA, on inhibitory neuron markers in the cortex, striatum, and hippocampus in rats.

The initial formation of the ganglionic eminence occurs at gestational day (GD) 10<sup>54</sup>, whereas interneurons (from the subventricular zone into the cortical plate) tangentially migrate from GD18 into the first postnatal weeks<sup>55,56</sup>. As the development of cortical inhibitory interneurons is a relatively protracted process, we hypothesised that the impact of gestational inflammation on inhibitory markers in different brain regions at adulthood would vary depending on the timing of MIA. Therefore, in the current study we investigated the effects of early gestation (GD10) or late gestation (GD19) polyI:C-induced MIA on gene expression of inhibitory indices (*GAD1*, *PVALB*, *SST*, and *SSTR2*) in the cortex, striatum, and hippocampus of adult male offspring. We hypothesised that late gestation polyI:C offspring would exhibit greater reductions in inhibitory mRNAs versus early gestation polyI:C offspring. Additionally, from previous investigations in polyI:C mouse offspring<sup>49</sup>, we hypothesised that polyI:C male offspring (GD10 and GD19 combined) have reduced *PVALB* mRNA in infralimbic cortex *a priori*. Finally, since inhibitory neurons transverse larger distances to reach the frontal cortex and hippocampus in comparison to the striatum, we hypothesised that polyI:C male offspring would exhibit more profound alterations in the cortex and hippocampus versus the striatum.

## Methods

**Animals and prenatal polyI:C administration.** Experiments were performed in accordance with the National Health and Medical Research Council's *Australian code for the care and use of animals for scientific purposes* (<https://www.nhmrc.gov.au/guidelines-publications/ea28>). The current study was approved by the University of Newcastle's Animal Care and Ethics Committee (Approval number A-2009-108). Rats were sourced from the University of Newcastle's Central Animal House and housed in conventional open-top cages with ad libitum food (standard rat chow, Specialty Feeds, WA, Australia) and water and 12 h light exposure in the University of Newcastle's Behavioral Sciences Animal Facility.

Nulliparous postnatal day (PND) 70–90 Wistar rats were time-mated and day of vaginal plug detection was designated as GD0. Pregnant rats were randomly assigned one of two timing groups: GD10 ( $n = 8$ ) or GD19 ( $n = 7$ ). On the appropriate GD, pregnant rats were weighed, lightly anesthetized with isoflurane, and injected intravenously through the tail vein with 0.1 M phosphate-buffered saline (PBS) (control;  $n = 8$ ) or 4 mg/mL of polyI:C (P9582, Sigma-Aldrich;  $n = 7$ ) in PBS at a volume of 1 mL/kg body weight. To confirm successful MIA, saphenous vein blood samples were collected 2 hours after treatment injections. Plasma was used for interleukin-6 (IL-6) measurement using rat IL-6 Quantikine ELISA (R&D Systems, MN, USA). PolyI:C treated dams had significantly increased IL-6 levels ( $624.7 \pm 57.0$  pg/mL) compared to saline-injected dams ( $68.4 \pm 57.0$  pg/mL) ( $F_{(1,8)} = 50.56$ ,  $p < 0.001$ ). There was no effect of gestational timing ( $F_{(1,8)} = 0.24$ ,  $p > 0.05$ ) or interaction between gestational timing and treatment ( $F_{(1,8)} = 0.23$ ,  $p > 0.05$ ) on maternal plasma IL-6 levels.

Offspring were weaned on PND 21, separated into same-sex cages in pairs. Male adult offspring from either treatment or timing group did not differ in weight at time of euthanasia (GD10 control:  $432 \pm 32$  g,  $n = 8$ ; GD19 control:  $441 \pm 44$  g,  $n = 8$ ; GD10 MIA:  $418 \pm 47$  g,  $n = 6$ ; GD19 MIA:  $415 \pm 28$  g,  $n = 6$ ; treatment:  $F_{(1,24)} = 1.74$ ,

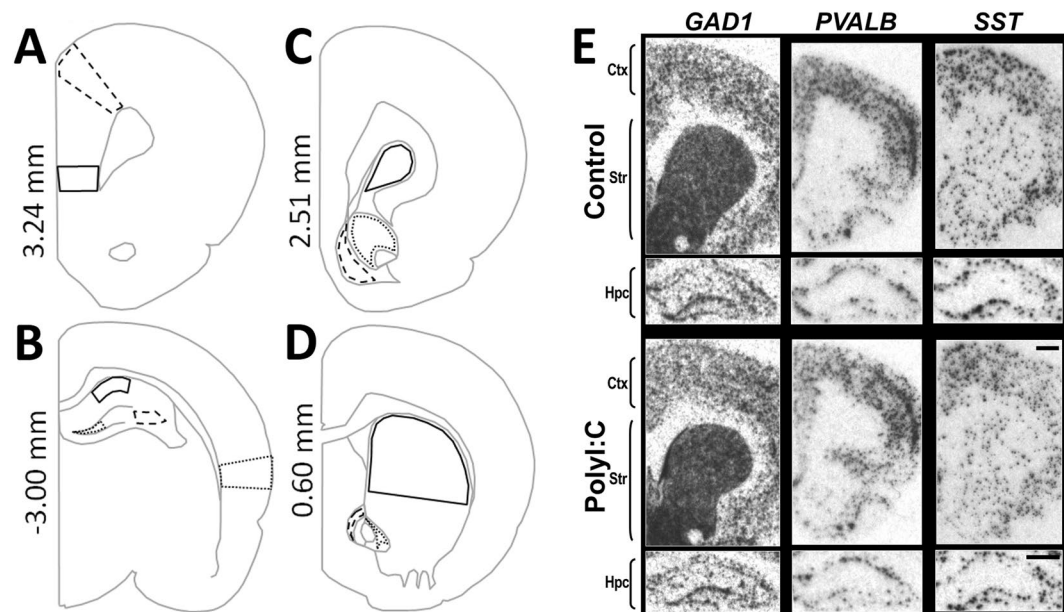


**Figure 1.** Gene expression of inhibitory-related markers quantified in cortex (Ctx), striatum (Str), and hippocampus (Hpc) subregions from representative *in situ* hybridization films when male offspring from vehicle (Control) or polyI:C (4 mg/kg) treated dams reached adulthood. (A–D) Grey line schematics of coronal sections of rat brain show the cortical (Ctx, A,B), striatal (Str, C,D), and hippocampal (Hpc, B) subregions (black outlines from  $-3.00$  to  $3.24$  mm bregma) that were quantified in this study. (A,B) In rostral (A) and caudal (B) cortical sections, three subregions were quantified: infralimbic (solid line), cingulate (dashed line), and auditory (dotted line on the right-most side) cortex. (B) In rostral hippocampal sections, three subregions were quantified: CA1 (solid line), CA3 (dashed line), and CA4 (dotted line). (C,D) In rostral (C) and middle (D) striatal sections, three subregions were quantified: dorsal striatum (solid line), nucleus accumbens core (dotted line), and nucleus accumbens shell (dashed line). (E) Representative autoradiographs of glutamate decarboxylase-1 (GAD1) mRNA, parvalbumin (PVALB) mRNA, and somatostatin (SST) mRNA *in situ* hybridization films from control and polyI:C offspring. Sections pictured are from postnatal day 70–81 offspring from the GD10 group. The representative Ctx and Str autoradiographs are from  $\sim 2.00$  mm bregma for GAD1 mRNA,  $2.50$  mm for PVALB mRNA, and  $1.70$  mm bregma for SST mRNA. The representative Hpc autoradiographs are from  $\sim -3.0$  mm bregma. Statistics of treatment effects and treatment  $\times$  subregion interactions are detailed in Table 1 and shown graphically in Fig. 4; there were no treatment  $\times$  timing interactions for any of the markers. Bregma level (mm) is indicated on the left of the schematics. Scale bar =  $1000\ \mu\text{m}$ .

Transcript	Brain region	Treatment		Treatment $\times$ Timing		Treatment $\times$ Subregion		Treatment $\times$ Timing $\times$ Subregion	
		F	p	F	p	F	p	F	p
GAD1	Cortex	0.001	0.97	0.912	0.349	0.403	0.61	1.709	0.2
	Striatum	0.099	0.755	0.092	0.764	0.601	0.469	0.247	0.66
	Hippocampus	0.56	0.461	2.213	0.15	0.846	0.416	0.428	0.614
PVALB	Cortex	2.868	0.106	0.012	0.914	0.241	0.741	0.843	0.418
	Striatum	3.286	0.084	0.127	0.725	1.15	0.321	0.29	0.721
	Hippocampus	3.716	0.066	0.484	0.494	0.879	0.415	3.176	0.056
SST	Cortex	<b>4.772*</b>	<b>0.043*</b>	0.078	0.783	<b>3.973*</b>	<b>0.035*</b>	0.089	0.89
	Striatum	<b>4.926*</b>	<b>0.036*</b>	2.33	0.14	<b>5.532*</b>	<b>0.012*</b>	1.072	0.338
	Hippocampus	0.279	0.602	0.324	0.575	0.129	0.825	2.248	0.132
SSTR2	Cortex	0.817	0.376	<b>4.533*</b>	<b>0.045*</b>	0.226	0.752	0.748	0.454
	Striatum	1.71	0.203	<b>4.508*</b>	<b>0.044*</b>	2.127	0.133	1.521	0.23
	Hippocampus	0.017	0.899	3.067	0.093	0.88	0.399	0.618	0.506

**Table 1.** Treatment effects and treatment interactions for inhibitory-related transcripts in cortex, striatum, and hippocampus. Two-way repeated measure ANOVAs [between-subject variables: treatment (control, polyI:C) and timing (GD10, GD19); within-subject variables: three subregions] were conducted per transcript per brain region. Significant values ( $p < 0.05$ ) are bold and accompanied with an asterisk (\*). Treatment effects for SST mRNA are shown in Figs. 1 and 2. Treatment  $\times$  timing interactions for SSTR2 mRNA are shown in Figs. 2 and 3. Treatment  $\times$  subregion interactions for SST mRNA are shown in Fig. 1 and Supplementary Fig. 3. \* $p < 0.05$ .

timing:  $F_{(1,24)} = 0.032$ , treatment  $\times$  timing:  $F_{(1,24)} = 0.18$ , all  $p > 0.05$ ). No more than two male offspring per litter were used in each experimental group to avoid litter-effect confounds and were randomly assigned to the study. Whole brains, snap-frozen in isopentane ( $-40^\circ\text{C}$ ) for storage ( $-80^\circ\text{C}$ ), were sectioned (coronal,  $14\mu\text{m}$ ) using a cryostat (Leica, Wetzlar, Germany) and mounted onto gelatin-coated glass slides.

**In situ hybridisation.** Riboprobes (Supplementary Table 1) were generated with  $^{35}\text{S}$ -UTP (CAT# NEG039H001MC Perkin Elmer, Waltham, Massachusetts, USA) using an *in vitro* transcription kit (CAT# P1121, Promega, Madison, Wisconsin, USA). *In situ* hybridisation was performed as previously described<sup>57</sup>, using 5 ng/ml radiolabelled riboprobes in hybridisation buffer, and  $^{35}\text{S}$ -UTP labelled sense strand riboprobes as a negative control (Supplementary Figures 1 and 2). Slides were exposed to BioMax MR (Kodak, Rochester, NY, USA) autoradiographic film (Supplementary Table 1) alongside a  $^{14}\text{C}$  standard slide (American Radiolabelled Chemicals, St. Louis, MO, USA).

**Quantification of mRNAs.** Developed films were digitised (600dpi, CAT# 8600 F, Canoscan, Canon Inc, Japan) and calibrated using NIH imaging software (v1.56; <http://rsb.info.nih.gov/nihi-image>) to produce nCi/mg tissue equivalent (t.e.) values based on the standard Rodbard curve obtained from the  $^{14}\text{C}$  standards to remove background intensity. Optical density values were quantitated using ImageJ (v1.48; <https://imagej.nih.gov/ij/>) and averaged across hemispheres from two to four sections per animal. Cortical [infralimbic (IL), cingulate (Cg), auditory (Aud), Fig. 1A,B], striatal [dorsal striatum (DS), nucleus accumbens core (AC), nucleus accumbens shell (AS), Fig. 1C,D], and hippocampal [cornu ammonis area 1 (CA1), cornu ammonis area 3 (CA3), cornu ammonis area 4 (CA4), Fig. 1B] regions were identified as per Paxinos 6<sup>th</sup> edition Rat Atlas<sup>58</sup>.

**Statistical analysis.** Graphs were plotted using Graph Pad Prism (v6) and data analysed with IBM SPSS statistics (v23). All data passed Shapiro-Wilk normality tests. Three-way mixed analysis of variance (ANOVA) was conducted for each region (cortex, striatum, and hippocampus), separately; hence there were three  $2 \times 2 \times 3$  repeated-measure (RM) ANOVAs in total. For each of these analyses, the two between-subject factors were treatment (polyI:C or vehicle) and timing (GD10 or GD19), and the within-subject factor was subregions (cortical subregions: IL, Cg, and Aud cortex; striatal subregions: DS, AC, and AS; hippocampal subregions: CA1, CA3, and CA4). Bonferroni tests were used for pairwise comparisons when the overall ANOVA was significant. The Greenhouse Geisser correction was used if Mauchley's sphericity test was violated for within-subjects interaction effects. Deming regressions were conducted to query the relationship between each offspring's regional gene expression of each marker and their respective maternal IL-6 protein exposure. Data are expressed as the mean  $\pm$  standard error of the mean (SEM) and two-sided  $p < 0.05$  was deemed statistically significant.

## Results

*GAD1* mRNA signals were punctate in the cerebral cortex and hippocampus, and darker and more homogeneous across the striatum (Fig. 1E). *PVALB* mRNA signals were punctate in the cerebral cortex, hippocampus, and striatum. *PVALB* mRNA signals in the cortex was stronger and denser in comparison to signals in the hippocampus and striatum (Fig. 1E). *SST* mRNA signals were punctate in all regions, and denser in the cerebral cortex in comparison to the hippocampus and striatum (Fig. 1E). *SSTR2* mRNA signals were highest in the molecular layer of the hippocampus, followed by the deeper layers of the cerebral cortex, the superficial layers of the cerebral cortex, and then the striatum (Fig. 2).

*GAD1* mRNA<sup>59,60</sup>, *PVALB* mRNA<sup>61</sup>, and *SST* mRNA<sup>62</sup> signals correspond to previously described distributions. Although cortical *SSTR2* mRNA signals were lighter in comparison to some studies<sup>63</sup>, the distribution corresponds to *SSTR2* mRNA and *SSTR2* binding results in multiple other studies (Supplementary Figure 1A)<sup>64–68</sup>. Control (sense) riboprobe hybridization, for all transcripts, was at background levels (Supplementary Figure 1B, 2).

There was a main effect of subregion on the expression pattern of *GAD1* mRNA, *PVALB* mRNA, *SST* mRNA, and *SSTR2* mRNA for cortical, striatal, and hippocampal comparisons in all offspring, except for *SST* mRNA in hippocampus (Supplementary Table 2). A summary of all treatment effects and treatment-related interactions are highlighted in Table 1. Briefly, there were significant treatment effects for *SST* mRNA in cortex (Fig. 3A) and striatum (Fig. 3B), treatment  $\times$  timing interactions for *SSTR2* mRNA in cortex (Fig. 3A) and striatum (Fig. 3B), and treatment  $\times$  subregion interactions for *SST* mRNA in cortex (Fig. 4A) and striatum (Fig. 4B). There were no significant treatment  $\times$  timing  $\times$  subregion interactions for any of the markers (Supplementary Figure 3A–C).

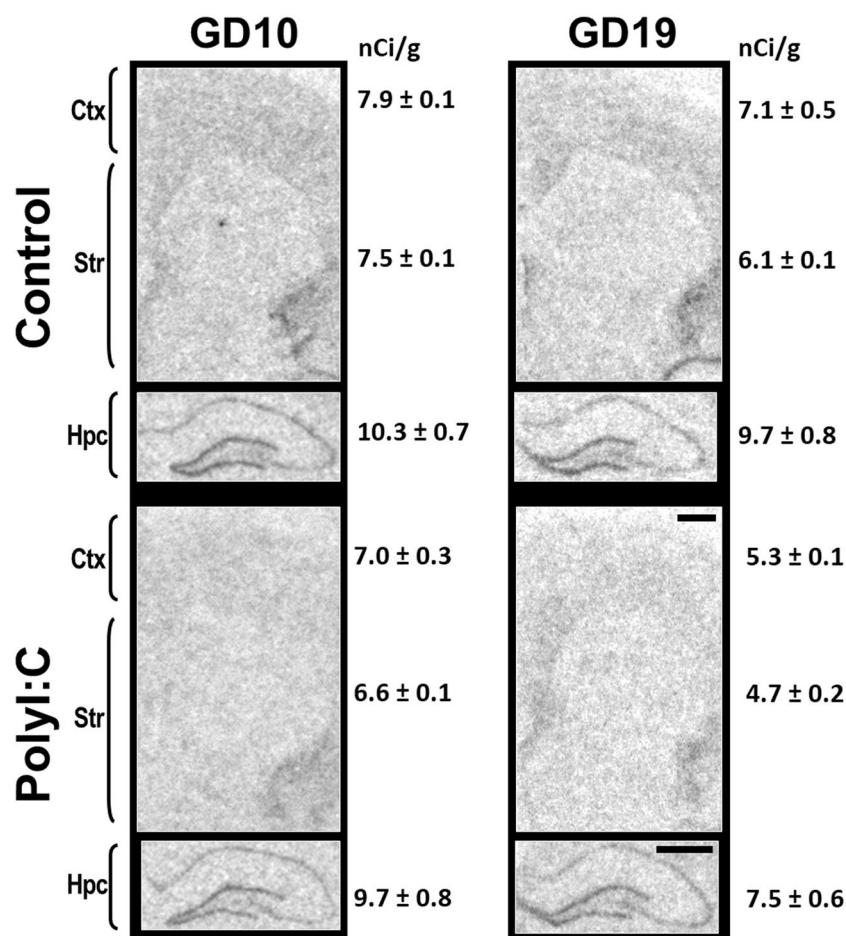
### Cortical *PVALB* mRNA and *SST* mRNA are reduced in polyI:C offspring in a subregion-specific manner, whereas cortical *SSTR2* mRNA is reduced in polyI:C offspring in a timing-specific manner.

*GAD1* mRNA was not changed by MIA exposure in cortex ( $F_{(1,24)} < 0.01$ ,  $p = 0.97$ ; Fig. 3A). Additionally, there were no treatment  $\times$  timing ( $F_{(1,24)} = 0.91$ ,  $p = 0.35$ ; Fig. 3A), treatment  $\times$  subregion (Fig. 4A) or treatment  $\times$  timing  $\times$  subregion ( $F_{(1,35,5)} < 1.0$ ,  $p > 0.05$ ; Supplementary Figure 3A) interaction effects on *GAD1* mRNA (Table 1).

There was no overall effect of MIA treatment ( $F_{(1,20)} = 2.87$ ,  $p = 0.11$ ; Fig. 3A) on *PVALB* mRNA in cortex. Additionally, there were no treatment  $\times$  timing ( $F_{(1,20)} = 0.01$ ,  $p = 0.91$ ; Fig. 3A), treatment  $\times$  subregion (Fig. 4A) or treatment  $\times$  timing  $\times$  subregion ( $F_{(1,40)} < 1.0$ ,  $p > 0.05$ ; Supplementary Figure 3A) interaction effects on *PVALB* mRNA (Table 1). As expected, *PVALB* mRNA was reduced by 22% in the IL cortex of polyI:C offspring (*a priori* univariate ANOVA:  $F_{(1,22)} = 5.08$ ,  $p = 0.04$ ; Fig. 4A).

There was a significant effect of MIA treatment on *SST* mRNA cortex, where polyI:C offspring had 20% less *SST* mRNA versus controls ( $F_{(1,17)} = 4.77$ ,  $p = 0.04$ ; Fig. 3A). There were no treatment  $\times$  timing ( $F_{(1,17)} = 0.08$ ,  $p = 0.78$ ; Fig. 3A) or treatment  $\times$  timing  $\times$  subregion ( $F_{(2,34)} = 0.09$ ,  $p = 0.92$ ; Supplementary Figure 3A) interaction effects on *SST* mRNA (Table 1). There was a treatment  $\times$  subregion interaction effect ( $F_{(2,34)} = 3.97$ ,  $p = 0.03$ ,





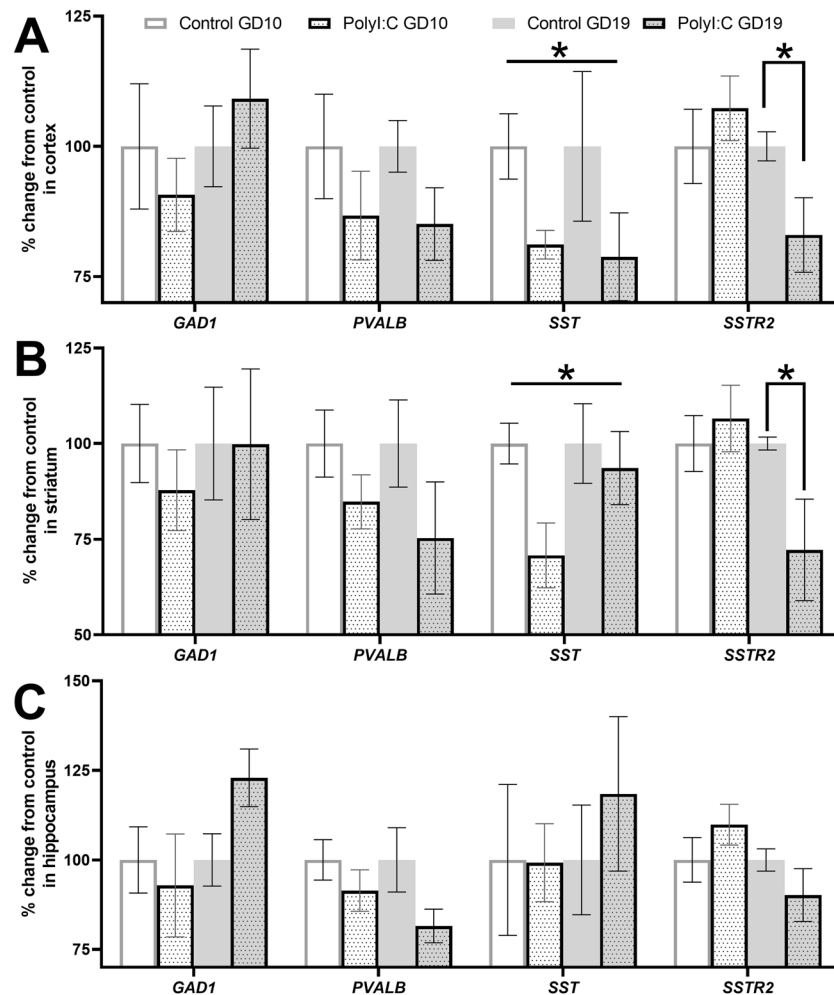
**Figure 2.** Representative autoradiographs of somatostatin receptor 2 (*SSTR2*) mRNA *in situ* hybridisation. Pregnant dams were treated with vehicle (Control, top) or 4 mg/kg polyriboinosinic:polyribocytidilic acid (PolyI:C, bottom) during early gestation (GD10, left) or late gestation (GD19, right). Coronal sections from ~2.3 mm bregma for cortex (Ctx) and striatum (Str), and ~3.0 mm bregma for hippocampus (Hpc) were processed when offspring reached adulthood. GD19 polyI:C offspring had significant reductions of *SSTR2* mRNA in cortex and striatum compared to controls. Sections pictured are from postnatal day 77–84 offspring. Statistics of treatment × timing interactions for *SSTR2* mRNA are shown in Table 1 and shown graphically in Fig. 3. Scale bar = 1000 μm. The values to the right of the figures denote the average signal intensity ± S.E.M. (nCi/g) of the three cortical [infralimbic (not visible on image), cingulate, auditory (not visible on image)], striatal (dorsal striatum, nucleus accumbens shell, nucleus accumbens core), and hippocampal (CA1, CA3, DG) subregions quantified from the animals portrayed in the representative autoradiographs.

Fig. 4A) where polyI:C offspring had 33% less *SST* mRNA in Cg cortex ( $F_{(1,17)} = 9.03$ ,  $p < 0.01$ ), but not in IL cortex ( $F_{(1,17)} = 0.19$ ,  $p = 0.67$ ) or in Aud cortex ( $F_{(1,17)} = 2.78$ ,  $p = 0.11$ ), compared to control offspring.

There was no overall effect of MIA on *SSTR2* mRNA in cortex ( $F_{(1,22)} = 0.82$ ,  $p = 0.38$ ; Fig. 3A). However, there was a significant treatment × timing interaction effect ( $F_{(1,22)} = 4.53$ ,  $p = 0.04$ ) where MIA offspring had 14% less *SSTR2* mRNA in cortex at GD19 ( $F_{(1,22)} = 4.49$ ,  $p < 0.05$ ; Fig. 3A grey dotted bars), but not GD10 ( $F_{(1,22)} = 0.77$ ,  $p = 0.39$ ; Fig. 3A white dotted bars), compared to controls (Fig. 3A white and grey solid bars). There were no treatment × subregion (Fig. 4A) or treatment × timing × subregion (Supplementary Figure 3A) interaction effects on *SSTR2* mRNA ( $F_{(2,44)} < 1.0$ ,  $p > 0.05$ , Table 1).

**Striatal *SST* mRNA is reduced in polyI:C offspring in a subregion-specific manner, whereas striatal *SSTR2* mRNA is reduced in polyI:C offspring in a timing-specific manner.** *GAD1* mRNA ( $F_{(1,24)} = 0.10$ ,  $p = 0.76$ ) and *PVALB* mRNA ( $F_{(1,22)} = 3.29$ ,  $p = 0.08$ ) were not affected in the striatum by MIA (Fig. 3B). There were no treatment × timing effects for *GAD1* mRNA ( $F_{(1,24)} = 0.09$ ,  $p = 0.76$ ) or *PVALB* mRNA ( $F_{(1,22)} = 0.13$ ,  $p = 0.73$ ) in striatum (Fig. 3B). There were also no treatment × subregion (Fig. 4B) or treatment × timing × subregion interaction effects (Supplementary Figure 3B) for *GAD1* mRNA ( $F_{(1,2,28,0)} < 1.0$ ,  $p > 0.05$ ) or *PVALB* mRNA ( $F_{(2,44)} < 1.15$ ,  $p > 0.05$ ; Table 1).

There was a significant effect of MIA treatment on *SST* mRNA striatum, where polyI:C offspring had 17% less *SST* mRNA versus controls ( $F_{(1,24)} = 4.93$ ,  $p = 0.04$ ; Fig. 3B). There were no treatment × timing ( $F_{(1,24)} = 2.33$ ,  $p = 0.14$ ; Fig. 3B) or treatment × timing × subregion ( $F_{(1,6,37,6)} = 1.07$ ,  $p = 0.35$ ; Supplementary Figure 3B)



**Figure 3.** Somatostatin receptor 2 (*SSTR2*) mRNA is decreased in offspring exposed to polyI:C on GD19, not GD10, in cortex and striatum. Pregnant dams were treated with vehicle (control, solid bar) or 4 mg/kg polyI:C, (dotted bar) during early gestation (GD10, white) or late gestation (GD19, grey). Glutamate decarboxylase-1 (*GAD1*), parvalbumin (*PVALB*), somatostatin (*SST*), and somatostatin receptor 2 (*SSTR2*) mRNAs were quantified in (A) cortex, (B) striatum, and (C) hippocampus from adult offspring. Data shown are pooled over three subregions for each region (cortex, striatum, and hippocampus). There was no overall treatment or treatment  $\times$  timing interaction effect for *GAD1* or *PVALB* mRNAs in any region. There was an overall treatment effect for *SST* mRNA in (A) cortex and (B) striatum, but not (C) hippocampus, (refer also to Table 1). There was a treatment  $\times$  timing interaction for *SSTR2* mRNA in (A) cortex and (B) striatum, but not (C) hippocampus, (refer also to Table 1). At GD10, there was no change in *SSTR2* mRNA levels observed between control and polyI:C offspring. At GD19, polyI:C offspring showed reduced *SSTR2* mRNA in (A) cortex by 29%, and in (B) striatum by 17% versus control offspring. Data are mean  $\pm$  SEM ( $n = 6-8$  rats per treatment and timing group). \* $p < 0.05$ .

interaction effect on *SST* mRNA. There was a treatment  $\times$  subregion interaction effect ( $F_{(1,6,37,6)} = 5.53, p < 0.01$ ) where polyI:C offspring had 29% less *SST* mRNA in the nucleus accumbens shell (AS) ( $F_{(1,24)} = 7.37, p = 0.01$ ; Fig. 4B), but not dorsal striatum (DS) ( $F_{(1,24)} = 0.366, p = 0.51$ ; Fig. 4B), compared to control offspring. The pairwise comparison of *SST* mRNA in the nucleus accumbens core (AC) did not reach significance ( $F_{(1,24)} = 3.89, p = 0.06$ ; Fig. 4B).

There was no overall effect of MIA on *SSTR2* mRNA in striatum ( $F_{(1,24)} = 1.71, p = 0.20$ ; Fig. 3B). However, there was a significant treatment  $\times$  timing interaction effect ( $F_{(1,24)} = 4.51, p = 0.04$ ) where MIA offspring had 33% less *SSTR2* mRNA in striatum at GD19 ( $F_{(1,24)} = 5.89, p = 0.02$ ; Fig. 3B), but not GD10 ( $F_{(1,24)} = 0.33, p = 0.57$ ; Fig. 3B), compared to controls. There were no treatment  $\times$  subregion (Fig. 4B) or treatment  $\times$  timing  $\times$  subregion (Supplementary Figure 3B) interaction effects on *SSTR2* mRNA ( $F_{(2,48)} < 2.13, p > 0.05$ , Table 1).

**Hippocampal gene expression of *GAD1*, *PVALB*, *SST*, or *SSTR2* is not altered in polyI:C offspring in a subregion- or timing-specific manner.** MIA exposure did not significantly alter *GAD1* mRNA ( $F_{(1,24)} = 0.56, p = 0.46$ ), *PVALB* mRNA ( $F_{(1,23)} = 3.72, p = 0.07$ ), *SST* mRNA ( $F_{(1,23)} = 0.28, p = 0.60$ ), or *SSTR2* mRNA ( $F_{(1,24)} = 0.24, p = 0.63$ ) in hippocampus (Fig. 3C). Further, there were no treatment  $\times$  timing

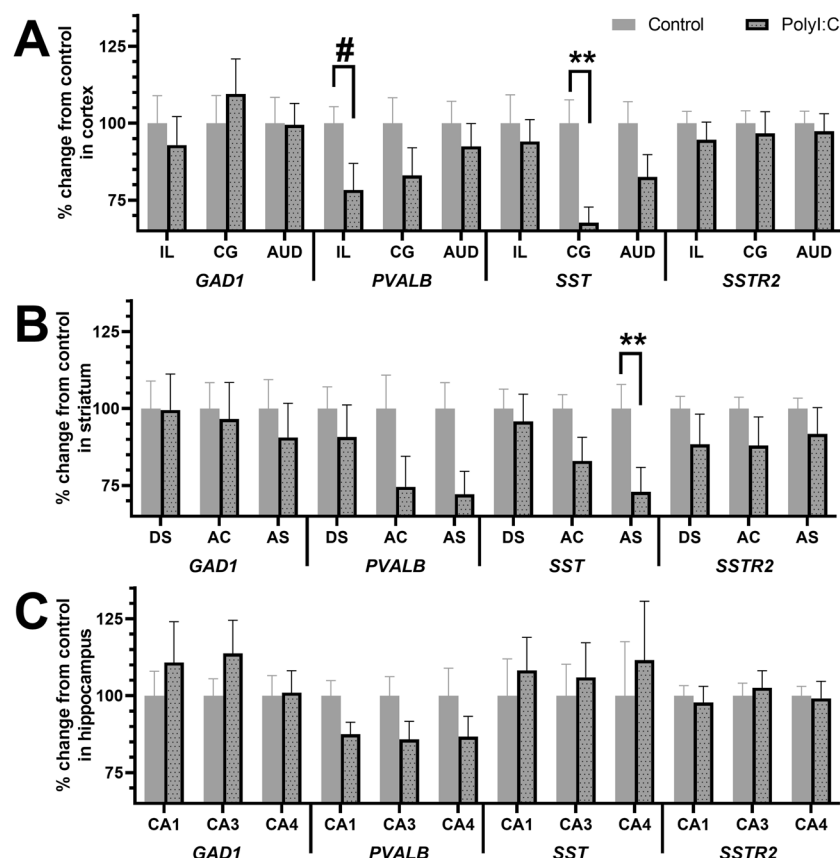


**Figure 4.** Inhibitory neuron gene expression is altered in subregions of (A) cortex and (B) striatum, but not (C) hippocampus, in adult male polyI:C offspring. Pregnant dams were treated with vehicle (Control, grey) or 4 mg/kg (PolyI:C, dotted) during either early gestation or late gestation (data herein represent gestational timing combined, data is presented separately in Supplementary Fig. 3). Glutamate decarboxylase 1 (*GAD1*) parvalbumin (*PVALB*), somatostatin (*SST*) and somatostatin receptor 2 (*SSTR2*) mRNAs were quantified in vehicle (control, grey bar) and polyI:C (dotted bar) offspring. Treatment  $\times$  subregion interaction effects were not present for *GAD1* or *SSTR2* mRNAs in any subregion. PolyI:C offspring had reductions in *PVALB* mRNA in the infralimbic cortex compared to controls (*a priori* univariate ANOVA:  $F(1, 22) = 5.08$ ,  $p = 0.04$ ). *SST* mRNA was significantly reduced in (A) cingulate cortex and (B) nucleus accumbens shell of the striatum in polyI:C offspring. Refer to Table 1 for treatment  $\times$  subregion interaction for *SST* mRNA. Data are mean  $\pm$  SEM ( $n = 12$ –16 rats per group). Infralimbic cortex (IL), cingulate cortex (CG), auditory cortex (AUD), dorsal striatum (DS), nucleus accumbens core (AC), nucleus accumbens shell (AS), cornu ammonis (CA). # $p < 0.05$ , \*\* $p < 0.01$ .

interaction effects for *GAD1* mRNA ( $F_{(1, 24)} = 2.21$ ,  $p = 0.15$ ), *PVALB* mRNA ( $F_{(1, 23)} = 0.48$ ,  $p = 0.49$ ), *SST* mRNA ( $F_{(1, 23)} = 0.32$ ,  $p = 0.58$ ), or *SSTR2* mRNA ( $F_{(1, 24)} = 2.62$ ,  $p = 0.12$ ) in hippocampus (Fig. 3C). Finally, there were no treatment  $\times$  subregion (Fig. 4C) or treatment  $\times$  timing  $\times$  subregion (Supplementary Figure 3C) interaction effects on *GAD1* mRNA (all  $F_{(1, 6, 39, 1)} < 0.85$ ,  $p > 0.05$ ), *PVALB* mRNA (all  $F_{(2, 46)} < 3.18$ ,  $p > 0.05$ ), *SST* mRNA (all  $F_{(1, 5, 35, 2)} < 2.25$ ,  $p > 0.05$ ), or *SSTR2* mRNA (all  $F_{(2, 48)} < 1.72$ ,  $p > 0.05$ ) in hippocampus (Table 1).

**Maternal IL-6 response to polyI:C treatment is related to *SST* mRNA in the cortex and striatum, but not hippocampus of offspring.** Across all offspring (treatment and timings combined), there was a significant negative relationship between maternal IL-6 protein two hours after treatment and adult offspring *SST* mRNA in cortex ( $F_{(1, 18)} = 4.39$ ,  $p = 0.05$ ) and striatum ( $F_{(1, 21)} = 9.59$ ,  $p < 0.01$ ), but not hippocampus ( $F_{(1, 20)} = 0.44$ ,  $p = 0.52$ ). The slopes were of moderate strength (cortex:  $R^2 = 0.196$ , striatum:  $R^2 = 0.314$ ; Supplementary Figure 4). No significant relationships were found between maternal IL-6 protein two hours after treatment and adult offspring *GAD1* mRNA (cortex:  $F_{(1, 21)} = 0.16$ , all  $p = 0.70$ ; striatum:  $F_{(1, 21)} = 0.19$ , all  $p = 0.67$ ; hippocampus:  $F_{(1, 21)} = 0.35$ ,  $p = 0.56$ ), *PVALB* mRNA (cortex:  $F_{(1, 17)} = 0.64$ ,  $p = 0.43$ ; striatum:  $F_{(1, 19)} = 2.58$ , all  $p = 0.12$ ; hippocampus:  $F_{(1, 20)} = 0.39$ ,  $p = 0.54$ ), or *SSTR2* mRNA (cortex:  $F_{(1, 21)} = 0.46$ ,  $p = 0.50$ ; striatum:  $F_{(1, 21)} = 1.74$ , all  $p = 0.20$ ; hippocampus:  $F_{(1, 21)} = 4.04$ ,  $p = 0.06$ ) levels in any brain region (Supplementary Figure 4).

## Discussion

Our findings demonstrate differential, long-term impacts of early gestation and late gestation MIA on inhibitory indices within the cortex and striatum of adult rat polyI:C offspring. As hypothesised, we found *PVALB* mRNA reductions in the infralimbic cortex of polyI:C offspring, which aligns with previous studies that report reductions in *PVALB*-positive cells in the medial prefrontal cortex in both early gestation and late gestation adult<sup>49,52</sup>

and juvenile<sup>53</sup> mouse polyI:C offspring. Somewhat surprisingly, we did not find significant changes in the inhibitory neuron marker, *GAD1* mRNA, in cortical subregions, and no significant changes in either *PVALB* or *GAD1* mRNAs in the hippocampus of polyI:C offspring. Although this lack of apparent change in *GAD1* mRNA aligns with the majority of the reports in polyI:C offspring, methodological variations may contribute to inconsistent findings in the field (see Supplementary Table 3 for a brief overview). We also report no significant changes in either *PVALB* or *GAD1* mRNA in the striatum. Although, to our knowledge, there have been no investigations of *PVALB* gene expression in the striatum of adult polyI:C offspring, our results align with studies that also find no significant change in *GAD1* mRNA in the striatum of GD14 polyI:C adult rat offspring<sup>38</sup>. Our findings suggest that some inhibitory neuron deficits may not consistently result from MIA, or may arise due to MIA at a different gestational time point. Further, we acknowledge that our sample size may not detect subtle changes. Indeed, we find approximate trend reductions in *PVALB* mRNA in the cortex ( $p < 0.11$ ), striatum ( $p < 0.09$ ) and hippocampus ( $p < 0.07$ ) of MIA offspring, and qualitative observation of our data suggests that this may arise from MIA at GD19. Our data suggests that future studies are warranted with larger sample sizes to investigate the effect of MIA timing on these inhibitory markers, particularly *GAD1* and *PVALB*.

We present the first report of reduced *SST* mRNA in both cortex and striatum in the rat MIA model of schizophrenia. In the cortex of people with schizophrenia, *SST* mRNA reductions are typically of a larger magnitude and can be as robust (if not more robust) than the more often studied *PVALB* mRNA changes<sup>8,20,21,24</sup>, with widespread decreases in *SST* mRNA reported in dlPFC, orbital frontal cortex, anterior cingulate cortex, motor cortex, and visual cortex<sup>8,20,21,24</sup>. The anatomically specific MIA-induced reductions in *SST* mRNA in the cingulate cortex, but not in infralimbic and auditory cortex, suggest that MIA may impact specific circuitry differentially. If MIA alone is not sufficient to recapitulate the fairly pervasive cortical reductions in *SST* mRNA observed in people with schizophrenia<sup>8,20,21,24,69</sup>, a subsequent postnatal stressor, or 'second hit', may be needed to elicit a widespread change in *SST* gene expression in the MIA model [see<sup>70</sup> for review]. The *SST* mRNA deficits detected in the cortex and striatum, but not hippocampus, may relate to the distinct origins of inhibitory neurons in these regions. In cortex, the majority of *PVALB*- and *SST*-containing inhibitory neurons are derived from the medial ganglionic eminence (MGE) (<sup>71</sup>, see<sup>72</sup> for review). In hippocampus, although some *PVALB*- and *SST*-containing inhibitory neurons also arise from the MGE, approximately 40% of *SST*-containing inhibitory neurons are derived from the caudal ganglionic eminence (CGE)<sup>73</sup>. The dominant period of MGE neurogenesis (GD9.5–GD13.5) precedes that of CGE neurogenesis (GD12.5–16.5)<sup>74,75</sup>. It is possible that the time points we chose to elicit MIA may alter neurogenesis for each ganglionic eminence distinctly and somewhat spare the interneurons destined for the hippocampus.

We also present the first report of cortical and striatal *SSTR2* mRNA reductions in a rodent MIA model of schizophrenia, which aligns with the *SSTR2* mRNA reduction seen in the cortex of people with schizophrenia<sup>26</sup>. Reductions in both regions, however, are contrary to our hypothesis that postulated that the cortex is more susceptible to MIA than the striatum. Given that our previous behavioural study showed working memory impairments in GD19 polyI:C offspring, but not GD10 polyI:C offspring<sup>50</sup>, and multiple studies show a central role of somatostatinergic signalling in cognitive function<sup>76–79</sup>, our present findings suggest that the combined *SSTR2* mRNA deficits in cortex and striatum (found only at GD19), in combination with the *SST* mRNA deficits in cortex and striatum, may contribute to the working memory deficits apparent in late gestation MIA offspring. Qualitative observation of our data shows that *SST* mRNA deficits in cortex in polyI:C offspring seem to occur at both GD10 and GD19, whereas *SST* mRNA deficits in striatum in polyI:C offspring seem driven by MIA at GD10. This is possibly evidence of a timing-specific effect of MIA in striatum but not cortex; however, we did not detect a significant treatment  $\times$  timing interaction effect or treatment  $\times$  timing  $\times$  subregion interaction effect that would permit us to investigate these further. Our data suggests that future studies are warranted with larger sample sizes may reveal significant effects of MIA timing on inhibitory markers in offspring.

Further, maternal IL-6 elevations are prolonged when polyI:C is administered in rodent dams during late gestation versus early gestation<sup>80</sup>, and maternal IL-6 levels in humans are associated with altered offspring neonatal functional connectivity and cognitive outcome<sup>81–84</sup>. Although we only measured maternal IL-6 at one time point, we also report a moderate negative relationship between maternal IL-6 and offspring *SST* gene expression in cortex and striatum. Overall, our data supports the notion that *SST* and *SSTR2* gene expression deficits may contribute to the working memory deficits apparent in late gestation MIA offspring.

Increased *SST*-positive interstitial white matter neurons (IWMN) and concurrent decreases in *SST* mRNA in the grey matter is reported in post-mortem frontal cortex from schizophrenia cases<sup>24,85</sup>. Recent studies show that both early gestation and late gestation polyI:C treatment increased the number of *SST*-positive IWMNs in regions that extend underneath the cingulate cortex in adult rat offspring<sup>86</sup>. Our detection of reduced *SST* mRNA in the grey matter suggests MIA during either the initial development of the ganglionic eminence<sup>54</sup>, or the time of neuronal tangential migration<sup>55,56</sup> could alter the migration or survival of *SST* cortical interneurons. Interestingly, late gestation polyI:C offspring exhibit increased *SST*-positive IWMNs in more extensive regions of white matter compared to early gestation polyI:C offspring<sup>86</sup>. Given that *SSTR2* is highly expressed on migrating neurons during early neurodevelopment in both rat and human<sup>87</sup>, our present findings may indicate a link between exaggerated IWMN pathology and *SSTR2* deficits in late gestation polyI:C offspring. Indeed, reductions in *SST* mRNA and reductions in *SSTR2* mRNA are correlated in dlPFC in schizophrenia<sup>26</sup>.

Overall, our current and prior findings are consistent with our hypothesis and earlier findings that gestational inflammation contributes to inhibitory neurotransmission deficits. This supports the growing evidence of altered inhibitory indices in the cortex and striatum of adult polyI:C offspring and recapitulates some aspects of neuropathology present in schizophrenia. We present the first rodent MIA study of cortical and striatal deficits in *SST* and *SSTR2* gene expression that concurs with cortical *SST* and *SSTR2* mRNA deficits found in post-mortem schizophrenia studies. Our novel finding of *SST* and *SSTR2* mRNA reductions in striatum suggests that further examination of *SST*-related neurotransmission may be warranted in the striatum of people with schizophrenia.



Although our data provide clues as to how inflammation, at different times during gestation, may contribute to schizophrenia-like pathologies, multiple gestational inflammatory insults and/or postnatal “second-hit” stressors are likely required to produce the large spectrum of symptoms and cognitive deficits that culminate in the diagnosis of schizophrenia. We postulate that somatostatinergic alterations could contribute to cognitive deficits previously reported in adult polyI:C offspring and in people with schizophrenia. Links between specific risk factors, such as maternal inflammation, and molecular alterations are critical to the development of mental illnesses, and we have identified SST and its receptor, SSTR2, as potential mediators of gestational inflammation-related risk for schizophrenia.

## Data availability

The data analysed during the current study are available from the corresponding author on reasonable request.

Received: 31 July 2019; Accepted: 26 December 2019;

Published online: 06 February 2020

## References

- Harrison, P. J. The neuropathology of schizophrenia. A critical review of the data and their interpretation. *Brain* **122**(Pt 4), 593–624 (1999).
- Powers, R. E. The neuropathology of schizophrenia. *J. Neuropathology Exp. Neurol.* **58**, 679–690 (1999).
- Bartley, A. F., Huang, Z. J., Huber, K. M. & Gibson, J. R. Differential activity-dependent, homeostatic plasticity of two neocortical inhibitory circuits. *J. Neurophysiol.* **100**, 1983–1994, <https://doi.org/10.1152/jn.90635.2008> (2008).
- Gibson, J. R., Bartley, A. F., Hays, S. A. & Huber, K. M. Imbalance of neocortical excitation and inhibition and altered UP states reflect network hyperexcitability in the mouse model of fragile X syndrome. *J. Neurophysiol.* **100**, 2615–2626, <https://doi.org/10.1152/jn.90752.2008> (2008).
- Hatanaka, Y., Zhu, Y., Torigoe, M., Kita, Y. & Murakami, F. From migration to settlement: the pathways, migration modes and dynamics of neurons in the developing brain. *Proc. Jpn. Academy. Ser. B, Phys. Biol. Sci.* **92**, 1–19, <https://doi.org/10.2183/pjab.92.1> (2016).
- Pelkey, K. A. *et al.* Hippocampal GABAergic Inhibitory Interneurons. *Physiol. Rev.* **97**, 1619–1747, <https://doi.org/10.1152/physrev.00007.2017> (2017).
- Marin, O., Anderson, S. A. & Rubenstein, J. L. Origin and molecular specification of striatal interneurons. *J. Neurosci.* **20**, 6063–6076 (2000).
- Fung, S. J. *et al.* Expression of interneuron markers in the dorsolateral prefrontal cortex of the developing human and in schizophrenia. *Am. J. Psychiatry* **167**, 1479–1488, <https://doi.org/10.1176/appi.ajp.2010.09060784> (2010).
- Dienel, S. J. & Lewis, D. A. Alterations in cortical interneurons and cognitive function in schizophrenia. *Neurobiol. Dis.* <https://doi.org/10.1016/j.nbd.2018.06.020> (2018).
- Volk, D. W. & Lewis, D. A. Early Developmental Disturbances of Cortical Inhibitory Neurons: Contribution to Cognitive Deficits in Schizophrenia. *Schizophr. Bull.* **40**, 952–957, <https://doi.org/10.1093/schbul/sbu111> (2014).
- Pinal, C. S. & Tobin, A. J. Uniqueness and redundancy in GABA production. *Perspect. developmental Neurobiol.* **5**, 109–118 (1998).
- Hu, J. S., Vogt, D., Sandberg, M. & Rubenstein, J. L. Cortical interneuron development: a tale of time and space. *Dev.* **144**, 3867–3878, <https://doi.org/10.1242/dev.132852> (2017).
- Hashimoto, T. *et al.* Alterations in GABA-related transcriptome in the dorsolateral prefrontal cortex of subjects with schizophrenia. *Mol. psychiatry* **13**, 147–161, <https://doi.org/10.1038/sj.mp.4002011> (2008).
- Fatemi, S. H., Earle, J. A. & McMenomy, T. Reduction in Reelin immunoreactivity in hippocampus of subjects with schizophrenia, bipolar disorder and major depression. *Mol. Psychiatry* **5**, 654–663, 571 (2000).
- Zhang, Z. J. & Reynolds, G. P. A selective decrease in the relative density of parvalbumin-immunoreactive neurons in the hippocampus in schizophrenia. *Schizophr. Res.* **55**, 1–10 (2002).
- Beckmann, H. & Lauer, M. The human striatum in schizophrenia. II. Increased number of striatal neurons in schizophrenics. *Psychiatry Res.* **68**, 99–109 (1997).
- Carlsson, A. *et al.* Interactions between monoamines, glutamate, and GABA in schizophrenia: new evidence. *Annu. Rev. Pharmacology Toxicol.* **41**, 237–260, <https://doi.org/10.1146/annurev.pharmtox.41.1.237> (2001).
- Guidotti, A. *et al.* Decrease in reelin and glutamic acid decarboxylase67 (GAD67) expression in schizophrenia and bipolar disorder: a postmortem brain study. *Arch. Gen. Psychiatry* **57**, 1061–1069 (2000).
- Curley, A. A. *et al.* Cortical Deficits of Glutamic Acid Decarboxylase 67 Expression in Schizophrenia: Clinical, Protein, and Cell Type-Specific Features. *The American journal of psychiatry*, <https://doi.org/10.1176/appi.ajp.2011.11010052> (2011).
- Hashimoto, T. *et al.* Conserved regional patterns of GABA-related transcript expression in the neocortex of subjects with schizophrenia. *Am. J. Psychiatry* **165**, 479–489, <https://doi.org/10.1176/appi.ajp.2007.07081223> (2008).
- Fung, S. J., Fillman, S. G., Webster, M. J. & Shannon Weickert, C. Schizophrenia and bipolar disorder show both common and distinct changes in cortical interneuron markers. *Schizophrenia Res.* **155**, 26–30, <https://doi.org/10.1016/j.schres.2014.02.021> (2014).
- Guillozet-Bongarts, A. L. *et al.* Altered gene expression in the dorsolateral prefrontal cortex of individuals with schizophrenia. *Mol. Psychiatry* **19**, 478–485, <https://doi.org/10.1038/mp.2013.30> (2014).
- Joshi, D., Fullerton, J. M. & Weickert, C. S. Elevated ErbB4 mRNA is related to interneuron deficit in prefrontal cortex in schizophrenia. *J. Psychiatr. Res.* **53**, 125–132, <https://doi.org/10.1016/j.jpsychires.2014.02.014> (2014).
- Joshi, D., Catts, V. S., Olaya, J. C. & Shannon Weickert, C. Relationship between somatostatin and death receptor expression in the orbital frontal cortex in schizophrenia: a postmortem brain mRNA study. *Npj Schizophrenia* **1**, 14004, <https://doi.org/10.1038/npschz.2014.4> (2015).
- Theodoropoulou, M. & Stalla, G. K. Somatostatin receptors: from signaling to clinical practice. *Front. neuroendocrinology* **34**, 228–252, <https://doi.org/10.1016/j.yfrne.2013.07.005> (2013).
- Beneyto, M., Morris, H. M., Rovinsky, K. C. & Lewis, D. A. Lamina- and cell-specific alterations in cortical somatostatin receptor 2 mRNA expression in schizophrenia. *Neuropharmacol.* **62**, 1598–1605, <https://doi.org/10.1016/j.neuropharm.2010.12.029> (2012).
- Brown, A. S. *et al.* Prenatal exposure to maternal infection and executive dysfunction in adult schizophrenia. *Am. J. Psychiatry* **166**, 683–690, <https://doi.org/10.1176/appi.ajp.2008.08010089> (2009).
- Buka, S. L. *et al.* Maternal infections and subsequent psychosis among offspring. *Arch. Gen. Psychiatry* **58**, 1032–1037 (2001).
- McGrath, J. J., Pemberton, M. R., Welham, J. L. & Murray, R. M. Schizophrenia and the influenza epidemics of 1954, 1957 and 1959: a southern hemisphere study. *Schizophrenia Res.* **14**, 1–8 (1994).
- Mednick, S. A., Machon, R. A., Huttunen, M. O. & Bonett, D. Adult schizophrenia following prenatal exposure to an influenza epidemic. *Arch. Gen. Psychiatry* **45**, 189–192 (1988).
- Mortensen, P. B. *et al.* Toxoplasma gondii as a risk factor for early-onset schizophrenia: analysis of filter paper blood samples obtained at birth. *Biol. Psychiatry* **61**, 688–693, <https://doi.org/10.1016/j.biopsych.2006.05.024> (2007).

32. Mortensen, P. B. *et al.* A Danish National Birth Cohort study of maternal HSV-2 antibodies as a risk factor for schizophrenia in their offspring. *Schizophr. Res.* **122**, 257–263, <https://doi.org/10.1016/j.schres.2010.06.010> (2010).
33. Piontkewitz, Y., Arad, M. & Weiner, I. Tracing the development of psychosis and its prevention: what can be learned from animal models. *Neuropharmacol.* **62**, 1273–1289, <https://doi.org/10.1016/j.neuropharm.2011.04.019> (2012).
34. Piontkewitz, Y., Arad, M. & Weiner, I. Risperidone administered during asymptomatic period of adolescence prevents the emergence of brain structural pathology and behavioral abnormalities in an animal model of schizophrenia. *Schizophrenia Bull.* **37**, 1257–1269, <https://doi.org/10.1093/schbul/sbq040> (2011).
35. Wolff, A. R. & Bilkey, D. K. The maternal immune activation (MIA) model of schizophrenia produces pre-pulse inhibition (PPI) deficits in both juvenile and adult rats but these effects are not associated with maternal weight loss. *Behavioural brain Res.* **213**, 323–327, <https://doi.org/10.1016/j.bbr.2010.05.008> (2010).
36. Zuckerman, L. & Weiner, I. Maternal immune activation leads to behavioral and pharmacological changes in the adult offspring. *J. Psychiatr. Res.* **39**, 311–323, <https://doi.org/10.1016/j.jpsychires.2004.08.008> (2005).
37. Bitanirhw, B. K. Y., Peleg-Raibstein, D., Mouttet, F., Feldon, J. & Meyer, U. Late prenatal immune activation in mice leads to behavioral and neurochemical abnormalities relevant to the negative symptoms of schizophrenia. *Neuropsychopharmacology* **35**, 2462–2478, <https://doi.org/10.1038/npp.2010.129> (2010).
38. Cassella, S. N. *et al.* Maternal immune activation alters glutamic acid decarboxylase-67 expression in the brains of adult rat offspring. *Schizophrenia Res.* **171**, 195–199, <https://doi.org/10.1016/j.schres.2016.01.041> (2016).
39. Richetto, J., Calabrese, F., Riva, M. A. & Meyer, U. Prenatal immune activation induces maturation-dependent alterations in the prefrontal GABAergic transcriptome. *Schizophrenia Bull.* **40**, 351–361, <https://doi.org/10.1093/schbul/sbs195> (2014).
40. Altar, C. A. *et al.* Anterograde transport of brain-derived neurotrophic factor and its role in the brain. *Nat.* **389**, 856–860, <https://doi.org/10.1038/39885> (1997).
41. Hashimoto, T. *et al.* Relationship of brain-derived neurotrophic factor and its receptor TrkB to altered inhibitory prefrontal circuitry in schizophrenia. *J. Neurosci.* **25**, 372–383, <https://doi.org/10.1523/jneurosci.4035-04.2005> (2005).
42. Glorioso, C. *et al.* Specificity and timing of neocortical transcriptome changes in response to BDNF gene ablation during embryogenesis or adulthood. *Mol Psychiatry* **11**, 633–648, <http://www.nature.com/mp/journal/v11/n7/supinfo/4001835s1.html> (2006).
43. Woo, N. H. & Lu, B. Regulation of cortical interneurons by neurotrophins: from development to cognitive disorders. *Neuroscientist: a Rev. J. bringing neurobiology, Neurol. psychiatry* **12**, 43–56, <https://doi.org/10.1177/1073858405284360> (2006).
44. Hemmerle, A. M. *et al.* Modulation of schizophrenia-related genes in the forebrain of adolescent and adult rats exposed to maternal immune activation. *Schizophr. Res.* **168**, 411–420, <https://doi.org/10.1016/j.schres.2015.07.006> (2015).
45. Baldan Ramsey, L. C., Xu, M., Wood, N. & Pittenger, C. Lesions of the dorsomedial striatum disrupt prepulse inhibition. *Neurosci.* **180**, 222–228, <https://doi.org/10.1016/j.neuroscience.2011.01.041> (2011).
46. Lee, A. S., Andre, J. M. & Pittenger, C. Lesions of the dorsomedial striatum delay spatial learning and render cue-based navigation inflexible in a water maze task in mice. *Front. Behav. Neurosci.* **8**, 42, <https://doi.org/10.3389/fnbeh.2014.00042> (2014).
47. Davies, D. A., Hurtubise, J. L., Greba, Q. & Howland, J. G. Medial prefrontal cortex and dorsomedial striatum are necessary for the trial-unique, delayed nonmatching-to-location (TUNL) task in rats: role of NMDA receptors. *Learn. Mem.* **24**, 262–266, <https://doi.org/10.1101/lm.044750.116> (2017).
48. Knuesel, I. *et al.* Maternal immune activation and abnormal brain development across CNS disorders. *Nature reviews. Neurol.* **10**, 643–660, <https://doi.org/10.1038/nrneurol.2014.187> (2014).
49. Meyer, U., Nyffeler, M., Yee, B. K., Knuesel, I. & Feldon, J. Adult brain and behavioral pathological markers of prenatal immune challenge during early/middle and late fetal development in mice. *Brain, behavior, Immun.* **22**, 469–486, <https://doi.org/10.1016/j.bbi.2007.09.012> (2008).
50. Meehan, C. *et al.* Effects of immune activation during early or late gestation on schizophrenia-related behaviour in adult rat offspring. *Brain, behavior, and immunity*, <https://doi.org/10.1016/j.bbi.2016.07.144> (2016).
51. Rahman, T. *et al.* Effects of Immune Activation during Early or Late Gestation on N-Methyl-D-Aspartate Receptor Measures in Adult Rat Offspring. *Front. Psychiatry* **8**, 77, <https://doi.org/10.3389/fpsy.2017.00077> (2017).
52. Han, M. *et al.* Intake of 7,8-Dihydroxyflavone During Juvenile and Adolescent Stages Prevents Onset of Psychosis in Adult Offspring After Maternal Immune Activation. *Sci. Rep.* **6**, 36087, <https://doi.org/10.1038/srep36087> (2016).
53. Matsuura, A. *et al.* Dietary glucoraphanin prevents the onset of psychosis in the adult offspring after maternal immune activation. *Sci. Rep.* **8**, 2158, <https://doi.org/10.1038/s41598-018-20538-3> (2018).
54. Sussel, L., Marin, O., Kimura, S. & Rubenstein, J. L. Loss of Nkx2.1 homeobox gene function results in a ventral to dorsal molecular respecification within the basal telencephalon: evidence for a transformation of the pallidum into the striatum. *Dev.* **126**, 3359–3370 (1999).
55. Anderson, S. A., Marin, O., Horn, C., Jennings, K. & Rubenstein, J. L. Distinct cortical migrations from the medial and lateral ganglionic eminences. *Dev.* **128**, 353–363 (2001).
56. Wichterle, H., Turnbull, D. H., Nery, S., Fishell, G. & Alvarez-Buylla, A. In utero fate mapping reveals distinct migratory pathways and fates of neurons born in the mammalian basal forebrain. *Dev.* **128**, 3759–3771 (2001).
57. Whitfield, H. J. Jr. *et al.* Optimization of cRNA probe *in situ* hybridization methodology for localization of glucocorticoid receptor mRNA in rat brain: a detailed protocol. *Cell. Mol. Neurobiol.* **10**, 145–157 (1990).
58. Paxinos, G. & Watson, C. *The Rat Brain in Stereotaxic Coordinates*. 6 edn, (Academic Press, 2007).
59. Gourfinkel-An, I. *et al.* Changes in GAD67 mRNA expression evidenced by *in situ* hybridization in the brain of R6/2 transgenic mice. *J. Neurochem.* **86**, 1369–1378 (2003).
60. Esclapez, M., Tillakaratne, N. J., Kaufman, D. L., Tobin, A. J. & Houser, C. R. Comparative localization of two forms of glutamic acid decarboxylase and their mRNAs in rat brain supports the concept of functional differences between the forms. *J. Neurosci.* **14**, 1834–1855 (1994).
61. Seto-Ohshima, A., Emson, P. C., Berchtold, M. W. & Heizmann, C. W. Localization of parvalbumin mRNA in rat brain by *in situ* hybridization histochemistry. *Exp. brain Res.* **75**, 653–658 (1989).
62. Fitzpatrick-McElligott, S., Card, J. P., Lewis, M. E. & Baldino, F. Jr. Neuronal localization of prosomatostatin mRNA in the rat brain with *in situ* hybridization histochemistry. *J. Comp. Neurol.* **273**, 558–572, <https://doi.org/10.1002/cne.902730410> (1988).
63. Stumm, R. K. *et al.* Somatostatin receptor 2 is activated in cortical neurons and contributes to neurodegeneration after focal ischemia. *J. Neurosci.* **24**, 11404–11415, <https://doi.org/10.1523/jneurosci.3834-04.2004> (2004).
64. Fehlmann, D. *et al.* Distribution and characterisation of somatostatin receptor mRNA and binding sites in the brain and periphery. *J. physiology, Paris* **94**, 265–281 (2000).
65. Hannon, J. P. *et al.* Somatostatin sst2 receptor knock-out mice: localisation of sst1–5 receptor mRNA and binding in mouse brain by semi-quantitative RT-PCR, *in situ* hybridisation histochemistry and receptor autoradiography. *Neuropharmacol.* **42**, 396–413, [https://doi.org/10.1016/S0028-3908\(01\)00186-1](https://doi.org/10.1016/S0028-3908(01)00186-1) (2002).
66. Faron-Górecka, A. *et al.* Chronic mild stress alters the somatostatin receptors in the rat brain. *Psychopharmacol.* **233**, 255–266, <https://doi.org/10.1007/s00213-015-4103-y> (2016).
67. Kong, H. *et al.* Differential expression of messenger RNAs for somatostatin receptor subtypes SSTR1, SSTR2 and SSTR3 in adult rat brain: analysis by RNA blotting and *in situ* hybridization histochemistry. *Neurosci.* **59**, 175–184 (1994).

68. Perez, J. *et al.* Localization of somatostatin (SRIF) SSTR-1, SSTR-2 and SSTR-3 receptor mRNA in rat brain by *in situ* hybridization. *Naunyn-Schmiedeberg's Arch. pharmacology* **349**, 145–160 (1994).
69. Volk, D. W. *et al.* Molecular mechanisms and timing of cortical immune activation in schizophrenia. *Am. J. psychiatry* **172**, 1112–1121, <https://doi.org/10.1176/appi.ajp.2015.15010019> (2015).
70. Feigenson, K. A., Kusnecov, A. W. & Silverstein, S. M. Inflammation and the Two-Hit Hypothesis of Schizophrenia. *Neurosci. Biobehav. Rev.* **38**, 72–93, <https://doi.org/10.1016/j.neubiorev.2013.11.006> (2014).
71. Nery, S., Fishell, G. & Corbin, J. G. The caudal ganglionic eminence is a source of distinct cortical and subcortical cell populations. *Nat. Neurosci.* **5**, 1279–1287, <https://doi.org/10.1038/nn971> (2002).
72. Butt, S. J. *et al.* The temporal and spatial origins of cortical interneurons predict their physiological subtype. *Neuron* **48**, 591–604, <https://doi.org/10.1016/j.neuron.2005.09.034> (2005).
73. Chittajallu, R. *et al.* Dual origins of functionally distinct O-LM interneurons revealed by differential 5-HT(3A)R expression. *Nat. Neurosci.* **16**, 1598–1607, <https://doi.org/10.1038/nn.3538> (2013).
74. Miyoshi, G., Butt, S. J., Takebayashi, H. & Fishell, G. Physiologically distinct temporal cohorts of cortical interneurons arise from telencephalic Olig2-expressing precursors. *J. Neurosci.* **27**, 7786–7798, <https://doi.org/10.1523/jneurosci.1807-07.2007> (2007).
75. Miyoshi, G. *et al.* Genetic fate mapping reveals that the caudal ganglionic eminence produces a large and diverse population of superficial cortical interneurons. *J. Neurosci.* **30**, 1582–1594, <https://doi.org/10.1523/jneurosci.4515-09.2010> (2010).
76. Abbas, A. I. *et al.* Somatostatin Interneurons Facilitate Hippocampal-Prefrontal Synchrony and Prefrontal Spatial Encoding. *Neuron* **100**, 926–939, <https://doi.org/10.1016/j.neuron.2018.09.029> (2018).
77. Prevot, T. D. *et al.* sst2-receptor gene deletion exacerbates chronic stress-induced deficits: Consequences for emotional and cognitive ageing. *Prog. Neuro-psychopharmacol. Biol. psychiatry* **86**, 390–400, <https://doi.org/10.1016/j.pnpbp.2018.01.022> (2018).
78. Boksa, P., Zhang, Y., Nouel, D., Wong, A. & Wong, T. P. Early Development of Parvalbumin-, Somatostatin-, and Cholecystokinin-Expressing Neurons in Rat Brain following Prenatal Immune Activation and Maternal Iron Deficiency. *Developmental Neurosci.* **38**, 342–353, <https://doi.org/10.1159/000454677> (2016).
79. Fee, C., Banasr, M. & Sibille, E. Somatostatin-Positive Gamma-Aminobutyric Acid Interneuron Deficits in Depression: Cortical Microcircuit and Therapeutic Perspectives. *Biol. Psychiatry* **82**, 549–559, <https://doi.org/10.1016/j.biopsych.2017.05.024> (2017).
80. Meyer, U. *et al.* The time of prenatal immune challenge determines the specificity of inflammation-mediated brain and behavioral pathology. *J. Neurosci.* **26**, 4752–4762, <https://doi.org/10.1523/jneurosci.0099-06.2006> (2006).
81. Spann, M. N., Monk, C., Scheinost, D. & Peterson, B. S. Maternal Immune Activation During the Third Trimester Is Associated with Neonatal Functional Connectivity of the Salience Network and Fetal to Toddler Behavior. *J. Neurosci.* **38**, 2877–2886, <https://doi.org/10.1523/jneurosci.2272-17.2018> (2018).
82. Rasmussen, J. M. *et al.* Maternal Interleukin-6 concentration during pregnancy is associated with variation in frontolimbic white matter and cognitive development in early life. *Neuroimage* **185**, 825–835, <https://doi.org/10.1016/j.neuroimage.2018.04.020> (2019).
83. Rudolph, M. D. *et al.* Maternal IL-6 during pregnancy can be estimated from newborn brain connectivity and predicts future working memory in offspring. *Nat. Neurosci.* **21**, 765–772, <https://doi.org/10.1038/s41593-018-0128-y> (2018).
84. Graham, A. M. *et al.* Maternal Systemic Interleukin-6 During Pregnancy Is Associated With Newborn Amygdala Phenotypes and Subsequent Behavior at 2 Years of Age. *Biol. Psychiatry* **83**, 109–119, <https://doi.org/10.1016/j.biopsych.2017.05.027> (2018).
85. Yang, Y., Fung, S. J., Rothwell, A., Tianmei, S. & Weickert, C. S. Increased interstitial white matter neuron density in the dorsolateral prefrontal cortex of people with schizophrenia. *Biol. Psychiatry* **69**, 63–70, <https://doi.org/10.1016/j.biopsych.2010.08.020> (2011).
86. Duchatel, R. J. *et al.* Increased white matter neuron density in a rat model of maternal immune activation - Implications for schizophrenia. *Prog. Neuro-psychopharmacol. Biol. psychiatry* **65**, 118–126, <https://doi.org/10.1016/j.pnpbp.2015.09.006> (2016).
87. Le Verche, V. *et al.* The somatostatin 2A receptor is enriched in migrating neurons during rat and human brain development and stimulates migration and axonal outgrowth. *PLoS One* **4**, e5509, <https://doi.org/10.1371/journal.pone.0005509> (2009).

## Acknowledgements

This study was supported by a National Health and Medical Research Council (NHMRC) project grant (APP1026070). CM is a recipient of an Australian Postgraduate Award (APA). US was supported by the Schizophrenia Research Institute (utilising infrastructure funding from the NSW Ministry of Health and NSW Ministry of Trade and Investment, Australia). CSW is funded by the NSW Ministry of Health, Office of Health and Medical Research and is a recipient of a National Health and Medical Research Council (Australia) Principal Research Fellowship (PRF) (#1117079). TR is supported by a Neuroscience Research Australia Scholarship.

## Author contributions

P.T.M., U.S., J.T., D.M.H., C.S.W. and T.R. conceived and designed the experiments. L.H., C.M. and T.R. undertook the experiments. T.R. analysed the data. T.R. and T.P.T. prepared the manuscript. All authors contributed to the interpretation of the data, edits, and approved the final manuscript.

## Competing interests

C.S.W. is on an advisory board for Lundbeck, Australia Pty Ltd and in collaboration with Astellas Pharma Inc., Japan. The other authors declare that they have no competing interests. Funding sources had no involvement in study design, in the writing of the report, or in the decision to submit the manuscript for publication. All authors declare that they have no competing financial or non-financial interests in relation to the work described in this report. The funding sources did not have any influence on the design, data collection, and analyses of these data in conjunction with this work, or the writing of this manuscript, or in the decision to publish this work.

## Additional information

**Supplementary information** is available for this paper at <https://doi.org/10.1038/s41598-020-58449-x>.

**Correspondence** and requests for materials should be addressed to T.P.-T.

**Reprints and permissions information** is available at [www.nature.com/reprints](http://www.nature.com/reprints).

**Publisher's note** Springer Nature remains neutral with regard to jurisdictional claims in published maps and institutional affiliations.



**Open Access** This article is licensed under a Creative Commons Attribution 4.0 International License, which permits use, sharing, adaptation, distribution and reproduction in any medium or format, as long as you give appropriate credit to the original author(s) and the source, provide a link to the Creative Commons license, and indicate if changes were made. The images or other third party material in this article are included in the article's Creative Commons license, unless indicated otherwise in a credit line to the material. If material is not included in the article's Creative Commons license and your intended use is not permitted by statutory regulation or exceeds the permitted use, you will need to obtain permission directly from the copyright holder. To view a copy of this license, visit <http://creativecommons.org/licenses/by/4.0/>.

© The Author(s) 2020